DALTON
FULL PAPER

Supramolecular interactions and magnetism of metal–radical chains †

Andrea Caneschi, Dante Gatteschi,* Nikolia Lalioti, Claudio Sangregorio and Roberta Sessoli

Department of Chemistry, University of Florence, Florence, Italy

Received 30th May 2000, Accepted 24th July 2000
First published as an Advance Article on the web 25th September 2000

The combination of organic imidazoline-1-oxyl-3-oxide radicals as building blocks with metal ions can yield 1-D magnetic chains in various conformations, depending on the metal ion and the 2 substituent of the radicals.

The interest in one-dimensional magnetic materials has been going through oscillations in the last few years, but on the whole they have long been the focus of high attention.[1–3] In fact they have the advantage of being both simple and complex, in such a way that many theories of statistical mechanics can find exact or quasi-exact solutions. At the beginning of the 1980s there was much attention devoted to spin diffusion effects observed in one-dimensional Heisenberg magnets.[4,5] Then attention switched to solitons,[6] solitary waves which can be observed in one dimensional ferro- and antiferro-magnets. Later, much excitement was aroused by the so-called Haldane conjecture.[7] This suggests that in one-dimensional antiferromagnets formed by integer spins, a gap is present between the lowest singlet state and the first excited state. Another interesting aspect of one-dimensional materials relates to observation of spin-Peierls transitions,[8] *i.e.* dimerization of the structure to be observed at low temperature, analogous to the dimerization observed in one-dimensional conductors (Peierls transition). In recent years it has been realized that Ising type one-dimensional magnets may show exciting possibilities of observing quantum admixed states.[9]

All these theoretical developments require experimental confirmations, therefore it is necessary to have available materials which can be considered as one-dimensional to a good approximation. Initially, examples were looked for among classic inorganic materials but in order to be considered as one-dimensional it is necessary that the inter-chain interactions are minimized. In a continuous solid this objective cannot be rigorously achieved, and molecular magnets may be better models as will be shown later. For a long time the best example of a one-dimensional antiferromagnet was provided by $[NMe_4]MnCl_3$ (TMMC),[10] in which the ratio between the intra- and the inter-chain interaction is of the order of 10^3, while in some molecular magnets it has been shown to be better than 10^4.[11,12]

Another important success has been achieved with molecular magnets in the first example of a one-dimensional ferrimagnet, an animal which was not previously present in the magnetic zoo.[13] Finally it should be recalled that the first clear example confirming the Haldane conjecture was found in the molecular system $Ni(en)_2(NO_2)ClO_4$, in which individual $Ni(en)_2^{2+}$ moieties with spin $S = 1$, are connected by bridging NO_2^- anions.[14,15] The interest in this field has not yet ceased, even if in recent years more attention has been devoted to attempts to synthesize bulk molecular magnets, which require the construction of three-dimensional architectures.

In this article we show how the design of one-dimensional materials can strongly benefit from the use of crystal engineering techniques, which can give rise to chains of different shapes, and how these differences can give rise to different properties. We will focus on chains constructed by assembling paramagnetic ligands and metal centers. The idea of using paramagnetic ligands is that they can give rise to strong magnetic interactions with the metal ions to which they bind. Further, another requirement is that the ligands must bridge two different metal ions in order to lead to chains. A suitable class of ligands fulfilling these conditions are the nitronyl nitroxides, 2-substituted-4,4,5,5-tetramethylimidazoline-1-oxyl-3-oxide radicals (NITR).[16,17] Such radicals are stable, and have the unpaired electron essentially delocalized on the two equivalent NO groups. These groups can be used to coordinate to two different metal ions. Since the two NO groups are equivalent, the magnetic interaction is transmitted from one side to the other of the molecule as if the ligand were a single atom with one unpaired electron. For the metal building blocks, metal(II) 1,1,1,5,5,5-hexafluoroacetylacetonates, $M^{II}(hfac)_2$ (M = Mn, Ni, Cu, Zn), are particularly well suited, since they have two vacant coordination sites which can be used to dock the radicals forming chains. Further the CF_3 groups are rather bulky and inefficient in transmitting magnetic interactions between chains, thus giving rise to ideal one-dimensional magnetic materials.[18] The manganese(II) derivatives for instance have been shown to have metal–radical antiferromagnetic exchange interactions with (J) in the range 200–400 K, which gives rise to one-dimensional ferrimagnetic behavior at relatively high temperatures. Eventually a cross-over to a three-dimensional magnetically ordered state occurs at 4–8 K, mainly as a consequence of dipolar interactions. Down to the cross-over to the magnetically ordered state, the chains behave as magnetic nanowires, and a large number of typically one-dimensional phenomena have been observed.

$Mn(hfac)_2(NITR)$ species are text-book examples of one-dimensional Heisenberg magnets, because the magnetic anisotropy of both the metal ions and the radicals is very low. From the structural point of view they are also very flexible, giving rise to several different structures.[19–24] The metal ions are hexa-coordinate, being coordinated to four oxygens from the two $hfac^-$ ligands and two oxygen atoms of two different NITR radicals. The aromatic NITR derivatives investigated are shown in Scheme 1.

The radicals bridge two different metal ions in a μ-1,5 fashion. Straight chains are formed if the radicals coordinate *trans* to each other, while if the coordination is *cis*, either zigzag chains[25] or trigonal helices are formed[26] (Scheme 2).

We are currently trying to obtain analogous compounds using magnetically anisotropic ions, such as cobalt(II), in order to explore how structural differences influence the magnetic

---

† Based on the presentation given at Dalton Discussion No. 3, 9–11th September 2000, University of Bologna, Italy.

Electronic supplementary information (ESI) available: rotatable 3-D crystal structure diagram in CHIME format. See http://www.rsc.org/suppdata/dt/b0/b004244g/

DOI: 10.1039/b004244g

Table 1 Structural parameters of one-dimensional compounds formed by the $M(hfac)_2$ and NITR building blocks

M	R	Configuration[a]	M–O[b]/Å	α[c]/°	d_1[d]/Å	β[e]/°	d_2[f]/Å	Ref.
Cu	Me	*trans*	2.4	0	3.23	—	—	27
Cu	Pr^i	*trans*	2.4	0	3.23	—	—	20
Cu	Pr^n	*trans*	2.4	0	3.21	—	—	28
Mn	Et	*cis*	2.13	50.7	3.8	—	—	12
Mn	Pr^n	*cis*	2.14	52.7	3.8	—	—	12
Mn	Pr^i	*trans*	2.17	29.3	5.6	—	—	11
Mn	C_6H_4OMe-*p*	helix	2.14	51.6	4.0	11.0/22.3	3.6/3.9	26
Mn	$C_6H_4NMe_2$-*p*	*cis*	2.18	60.6	3.8	14.7/30.7	3.7/4.2	34
Mn	C_6H_4Me	*cis*	2.11	51.6	3.7	15.8/25.3	3.7/4.1	This work
Co	C_6H_4OMe-*p*	helix	2.1	62.9	3.8	10.1/9.6	3.6/3.9	This work
Co	C_6H_4Me-*p*	helix	2.1	68.2	3.8	5.6/8.4	3.8/3.6	This work

[a] *trans* Corresponds to a straight chain, *cis* to a zigzag chain, helix to a trigonal helix. [b] Average distance between the metal and the radical oxygen atom. [c] Angle between two hfac planes. [d] Distance between the centroids of the hfac ligands considered as five membered rings. [e] Angle between the phenyl and hfac planes. [f] Distance between the centroids of the hfac and phenyl planes.

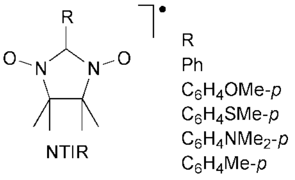

Scheme 1

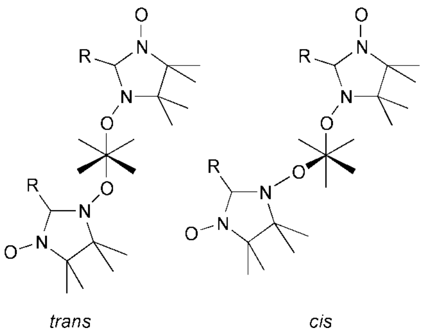

Scheme 2

properties. In this case the control of the spatial arrangement of the magnetic building blocks is of paramount importance in determining the strength of the magnetic interaction. The possibility of controlling the shape of the chains depends on the coordination bond between the metal ion and the radicals and on supramolecular interactions such as stacking interactions involving π orbitals in the organic moieties. We decided therefore to explore how the R substituents of the NITR radicals influence the structure of the chains, and report here some new crystal structures, in order to elucidate the factors determining the shape of the chains which also determines their packing in the crystal. As the magnetic ordering in this class of materials seems to be driven by inter-chain dipolar interactions, the packing is expected to significantly affect the ordering phenomenon, and in particular, transition temperatures.

Structural aspects

The role of the substituent R is of great importance in determining the nature of the chain which is formed, but also the nature of the metal ion is important. Indeed, for copper(II) only straight chains have been reported so far (Table 1). Since the radical is the weak ligand in the coordination environment of copper(II) the NO groups tend to occupy the axially elongated positions of the distorted octahedron typical for this Jahn–Teller active ion and all reported structures of copper(II) chains correspond to *trans* coordination of the NITR ligands, with long metal–oxygen bond distances of *ca.* 2.4 Å.[20,27–30] In this case, therefore, the steric requirements of the metal ions are the driving force determining the type of chains which can be obtained. For other metal ions, such as manganese(II) or cobalt(II) which are not so sterically demanding this is not so. The former is the ion for which most structures, both one-dimensional and oligonuclear, have been reported.[11,12,31–33] For R = Et[12] or Pr^n,[12] the coordination of the nitroxides around the metal ion is *cis* and the chains are zigzag, while with R = Pr^i,[11] the coordination is *trans* and the chains are straight. The most obvious explanation is that the more bulky isopropyl group prefers the less sterically hindered *trans* configuration; *cis* coordination is observed also in a mononuclear bis-NITMe complex.[31]

We checked also the possibility of stacking interactions between the planes of the hfac ligands, measuring the angle between the planes (α) and their separation (d_1). Since, in general, the planes are not parallel to each other we define the distance between the planes as the distance between the centroids of the hfac ligands considering them as five membered rings. For the Co and Mn derivatives, $d = 3.8$ and 5.6 Å while α ranges from 29 to 53°, indicating that the interactions are small or negligible. Presumably such interactions have no major role in defining the structure of the chains of the manganese and cobalt complexes.

However, when the R group contains phenyl rings clear stacking interactions are observed between the phenyl and the hfac planes. Here, we use two parameters to define the stacking interaction, namely the angle between the planes (β) and the distance between the centroids (d_2). In the oligonuclear[19] $[Mn(hfac)_2(NITPh)]_6$ the angle between the planes is 8° and their separation is 3.4 Å. In the corresponding bis-NITPh mononuclear compound no significant stacking interaction is observed.[31] Chains with aromatic substituted radicals may be developed as zigzag and/or as helices. For the latter, the space group is hexagonal which can lead to stacking interactions between each phenyl ring and two adjacent hfac planes thus forming an asymmetric 'sandwich structure' with the phenyl ring between the two hfac planes.

$Mn(hfac)_2(NITC_6H_4OMe$-*p*$)$[26] was reported to have a helical structure, with spontaneous resolution from solution. The stronger stacking interaction is defined by $\beta = 11°$, and $d_2 = 3.6$ Å while the other is much weaker ($\beta = 22.3°$, $d_2 = 3.9$ Å). We have now obtained the analogous cobalt(II) derivative $Co(hfac)_2(NITC_6H_4OMe$-*p*$)$ **1**. Again, a trigonal helix is spontaneously resolved, with a unit cell isomorphous to the manganese analogue. The stacking interactions are stronger in the cobalt(II) derivative relative to the manganese(II) derivative with the stronger interaction being characterized by $\beta = 10.1°$ and d_2 3.6 Å, while the weaker interaction has $\beta = 9.6°$ and $d_2 = 3.9$ Å.

In order to check if the formation of helices is related to the presence of stacking interactions involving phenyl rings, we decided to investigate other NITR radicals. While no suitable

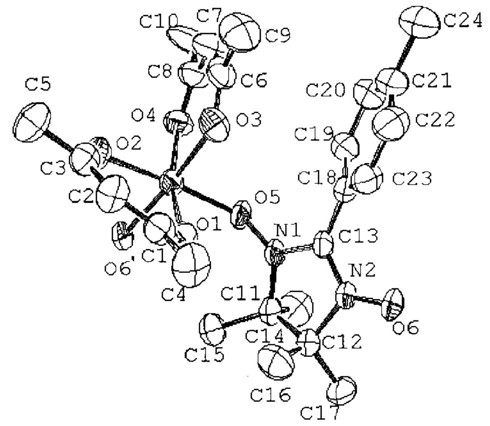

Fig. 1 ORTEP view of the asymmetric unit of Co(hfac)$_2$(NITC$_6$H$_4$-Me-*p*) **2**. The fluorine atoms are omitted for clarity.

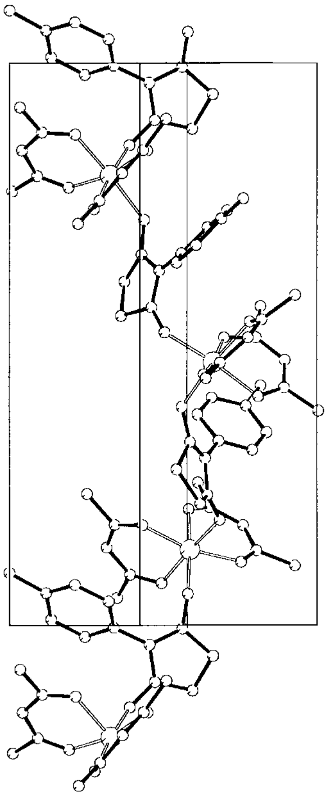

Fig. 2 Simplified view of the unit cell contents of Co(hfac)$_2$-(NITC$_6$H$_4$Me-*p*) **2**. The chain develops along the unique axis *c*.

crystals were obtained with the NITPh radical NITC$_6$H$_4$Me-*p* provided crystals suitable for a X-ray analysis. Co(hfac)$_2$-(NITC$_6$H$_4$Me-*p*) **2** like **1**, spontaneously resolved from solution and a trigonal helix was formed. The space group of the crystal was $P3_2$, while that of the previous helices was $P3_1$, however, the size of the unit cell was essentially the same. The structure of Co(hfac)$_2$(NITC$_6$H$_4$Me-*p*) **2** consists of octahedrally coordinated cobalt(II) ions comprising four oxygen atoms of two hfac molecules and two oxygen atoms from two *cis* coordinated NITC$_6$H$_4$Me-*p* radicals defining the coordination polyhedron. The asymmetric unit is shown in Fig. 1 with the oxygen atoms of the radicals bound to adjacent cobalt atoms thus bridging the Co(hfac)$_2$ units and forming a one-dimensional polymer. The chains form a helix, as demanded by the crystallographic 3_2 symmetry, parallel to the crystallographic axis *c* as shown in Fig. 2. The coordination polyhedron of each Co(II) ion is rather distorted with Co–O distances ranging from 2.027(4) to 2.120(4) Å while the maximum distortion from octahedral symmetry is observed in the O1–Co–O4 angle which is 166.3(2)°. This distortion can be explained in terms of the *cis* coordination of the two radicals and to the π-stacking interactions between the phenyl ring of the NITC$_6$H$_4$Me-*p* radical and the unsaturated region of the nearest hfac molecules. The stacking interactions between the corresponding planes are characterized by the angles $\beta = 5.6$ and 8.4° and the distances $d_2 = 3.8$ and 3.6 Å, respectively (Table 1). The stacking interactions appear to be slightly stronger here than in the Co-(hfac)$_2$(NITC$_6$H$_4$OMe-*p*) derivative in agreement with the higher electron density expected on the phenyl ring.

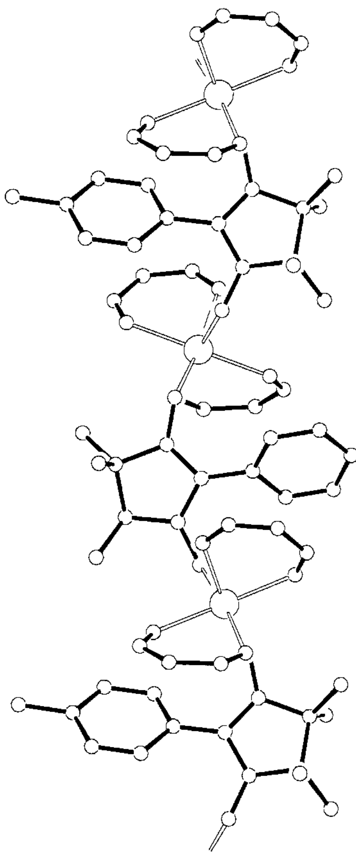

Fig. 3 Simplified view of the chains running along the *b* axis in Mn(hfac)$_2$(NITC$_6$H$_4$Me-*p*)·0.25CHCl$_3$ **3**.

Attempts were also made to crystallize the analogous manganese(II) derivative. Crystals suitable for X-ray analysis were obtained by using a 1 : 4 mixture of CHCl$_3$ and *n*-heptane. The compound crystallizes in the monoclinic *C*2/*c* space group with cell parameters which are very similar to that of Mn(hfac)$_2$-(NITC$_6$H$_4$NMe$_2$-*p*) [$a = 28.183(4)$, $b = 13.899(2)$, $c = 23.425(5)$ Å, $\beta = 125.28(1)$°]. The structure of Mn(hfac)$_2$(NITC$_6$H$_4$Me-*p*) **3** consists of chains developing along the *b* axis with the radical *cis* coordinated to the metal ion. In **3** π-stacking occurs between the phenyl ring and one hfac ligand without formation of a 'sandwich' structure as shown in Fig. 3.

In the helical compounds the space group is hexagonal and each chain is surrounded by six equivalent chains at 11.131 Å in the Mn(hfac)$_2$(NITC$_6$H$_4$OMe-*p*) **4**, at 11.289 Å in **1** and at 11.260 Å in **2**, this being estimated as the shortest interchain M(II)–M(II) contact. In compound **3** the space group is monoclinic and each chain is surrounded by other six chains at distances ranging from 11.028 to 15.350 Å.

The crystal packing of the helices formed in **1** and **2** and that of zigzag chains present in **3** are shown in Fig. 4, where a simplified view of the metal coordination spheres and of the bridging ONCNO moieties are viewed along the chain.

In conclusion, it is possible to control the stereochemistry of linear chains formed by M(hfac)$_2$ and NITR building blocks, by taking advantage of the nature of the metal ion and the stacking interactions between the aromatic rings and the hfac planes.

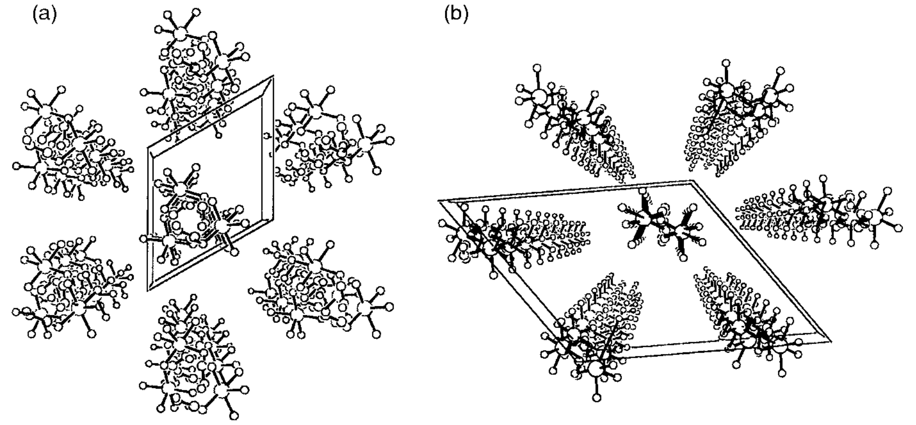

Fig. 4 The crystal packings of the helix formed in **2** (a) and that of zigzag chains present in **3** (b). A simplified view of the metal coordination spheres and of the bridging ONCNO moieties are viewed along the chain.

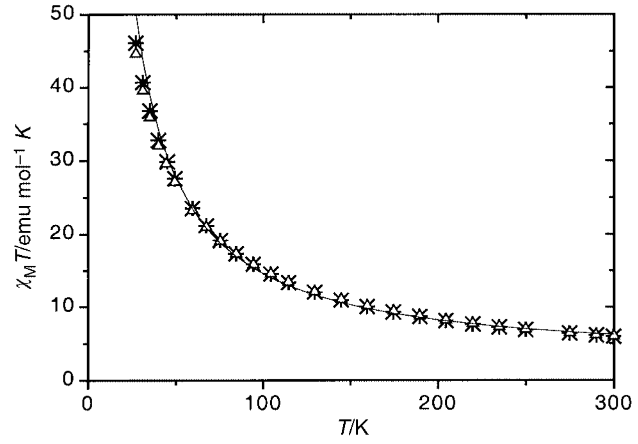

Fig. 5 Temperature dependence of χT per mol of metal–radical units for Mn(hfac)$_2$(NITC$_6$H$_4$OMe-*p* **4**) (Δ) and Mn(hfac)$_2$(NITC$_6$H$_4$Me-*p* **3**) (*) measured with a magnetic field $H = 0.1$ T. The solid line corresponds to the best fit of the experimental points above 50 K (see text).

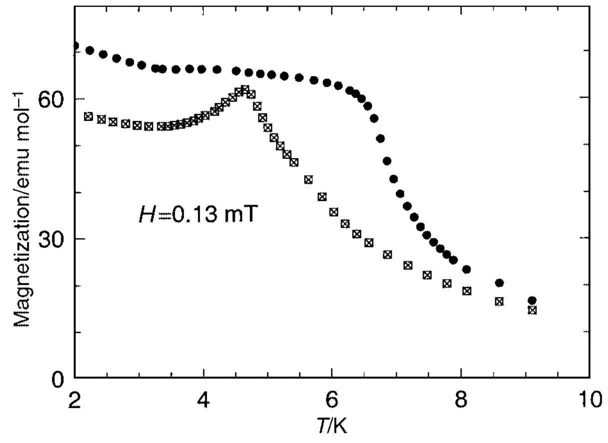

Fig. 6 Low-temperature dependence of the magnetization in low applied field for Mn(hfac)$_2$(NITC$_6$H$_4$OMe-*p*) **4** (×) and Mn(hfac)$_2$(NITC$_6$H$_4$Me-*p*) **3** (●).

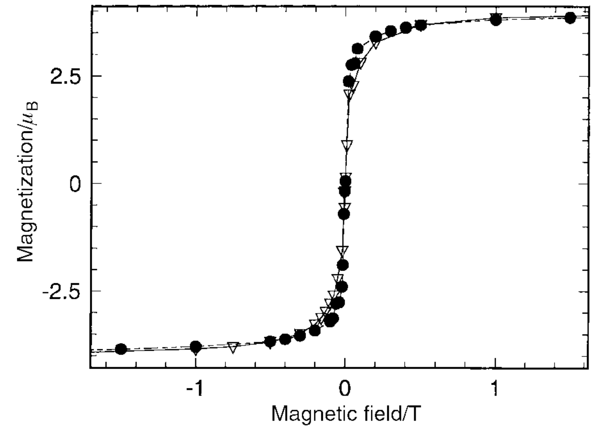

Fig. 7 Field dependence of the magnetization of Mn(hfac)$_2$(NITC$_6$H$_4$OMe-*p*) **4** (●) and Mn(hfac)$_2$(NITC$_6$H$_4$Me-*p*) **3** (∇), measured at 2.5 and 3.0 K respectively.

However the preference for one form over another is not very strong, and it is possible to change from one to the other through slight changes in the experimental conditions.

Magnetic properties

The magnetic properties of Mn(hfac)$_2$(NITC$_6$H$_4$OMe-*p*) **4** have been previously reported.[26] The temperature dependence of χT for Mn(hfac)$_2$(NITC$_6$H$_4$Me-*p*) **3** is shown in Fig. 5, together with that of Mn(hfac)$_2$(NITC$_6$H$_4$OMe-*p*) **4** for comparison. The two sets of data are practically identical in the range 20–300 K. The temperature dependence of χT shows a continuous increase on lowering the temperature and reaches very high values at low temperatures. This behavior is typical of one-dimensional ferrimagnets, where the non-compensation of the spin $S = 5/2$ of the metal ion and $S = 1/2$ of the radical leads to an increasing magnetic moment as the correlation length increases on decreasing the temperature. The data can be well fitted with a model which treats the manganese(II) spins, $S = 5/2$, as classical spins, and those of the radicals, $S = 1/2$, as quantum spins.[35] The value of the coupling constant for both **3** and **4** is 368(3) cm^{-1}, in good agreement with values previously reported for similar compounds.[11,12] The fact that the magnetic behavior of the two compounds is identical in the paramagnetic phase is in accord with the similar coordination environment of the manganese(II) as well as the spin density on the radical. In order to clearly reveal the presence of transitions to three dimensional magnetic ordering the low field ($H = 0.13$ mT) magnetization of **3** and **4** was measured and the results are plotted in Fig. 6. The two compounds show a divergence followed by a leveling of the magnetization but the critical temperatures, estimated here by measuring the point of maximum slope, are significantly different, $T = 4.8$ K for Mn(hfac)$_2$(NITC$_6$H$_4$OMe-*p*) **4** and 6.8 K for Mn(hfac)$_2$(NITC$_6$H$_4$Me-*p*) **3**. The magnetically ordered state corresponds to a ferromagnetic alignment of the ferrimagnetic chains, as confirmed by the magnetization curves of the two compounds, which show a rapid saturation of the magnetization to a value of 4 μ_B (Fig. 7), as expected for $S = 2$ for the manganese–radical pair.

The coercive field does not exceed 1 mT confirming the soft magnetic character of these kind of materials owing to the very low magnetic anisotropy, which leads to an almost completely reversible motion of the domains' walls.

Given the great similarity of the behavior in the paramagnetic phase the difference in the ordering temperature of the two compounds must arise from the different secondary structures of the chains, namely zigzag for Mn(hfac)$_2$(NITC$_6$H$_4$Me-*p*) **3** and trigonal helix for Mn(hfac)$_2$(NITC$_6$H$_4$OMe-*p*). The lower symmetry for the former leads to the presence of two closer chains and this presumably stabilizes the dipolar ferromagnetic alignment along this direction, with a sizeable increase in T_c, compared to the equivalence of the *ab* plane in the trigonal structures. Single crystal magnetic characterizations of the two compounds are in progress to confirm this hypothesis. This is a clear indication of how minor structural changes can induce large differences in the magnetic properties according to the critical temperature, which increases by *ca.* 50% from **4** to **3**.

Preliminary magnetic measurements on the cobalt(II) derivatives show an one-dimensional ferrimagnetic behavior in the paramagnetic phase, with evidence of anomalous magnetization at low temperature. The introduction of magnetic anisotropy in the interaction associated with the presence of high-spin cobalt(II) gives rise to a much more complex behavior, which requires a full characterization of the magnetic anisotropy through single crystal magnetic studies, which are in progress.

Syntheses

Co(hfac)$_2$(NITC$_6$H$_4$OMe-*p*) **1** and Co(hfac)$_2$(NITC$_6$H$_4$Me-*p*) **2** were synthesized using the same procedure: 1 mmol of the Co(hfac)$_2$·2H$_2$O was dissolved in 60 ml of dry boiling *n*-heptane, and a solution of 1 mmol of the radical in 10 ml of dry *n*-heptane was added. The final solution was allowed to cool to room temperature and stored at 4 °C. Dark green well developed hexagonal prismatic crystals suitable for X-ray determination were collected after 3 days and well analysed for Co(hfac)$_2$(NITC$_6$H$_4$OMe-*p*) **1** and for Co(hfac)$_2$(NITC$_6$H$_4$Me-*p*) **2**. Anal. Calc. for $C_{24}F_{12}CoH_{21}N_2O_7$ **1**: C, 39.15; H, 2.87; N, 3.83. Found: C, 39.03; H, 2.97; N, 3.67. Calc. for $C_{24}F_{12}CoH_{21}N_2O_6$ **2**: C, 40.02; H, 2.94; N, 3.89. Found: C, 39.93; H, 3.01; N, 3.82%.

Mn(hfac)$_2$(NITC$_6$H$_4$Me-*p*)·0.25CHCl$_3$ **3** was prepared by dissolving 1 mmol of Mn(hfac)$_2$·2H$_2$O in 10 ml of CHCl$_3$, and a solution of 1 mmol of the NITC$_6$H$_4$Me-*p* radical in 40 ml of dry *n*-heptane was added. The resulting solution was allowed to stand at ambient temperature for slow evaporation and dark green elongated crystals were obtained after 12 h. Destruction of the crystal structure was observed after exposure of the crystals to air. The assumption that the crystals retained some chloroform was in accord with the elemental analysis values. Calc. for $C_{24}F_{12}MnH_{21}N_2O_6 \cdot 0.25CHCl_3$: C, 39.03; H, 2.87; N, 3.75. Found: C, 39.16; H, 2.80; N, 3.79%.

Crystallography

X-Ray diffraction data were collected on an Enraf-Nonius CAD4 four-circle diffractometer. Corrections for Lorentz and polarization effects and for absorption (ψ-scan) were applied. The crystal structures of the three compounds were solved by direct methods using the SIR92 program,[36] which, in all cases, gave the position of all non-hydrogen atoms but few fluorine atoms which were later identified by successive Fourier difference syntheses. Refinements were carried out on F^2 by full-matrix least-square techniques, using the SHELXL-93 program package.[37] The hydrogen atoms were calculated at fixed distances and refined with an overall isotropic thermal parameter. Owing to the destruction of the crystal after exposure to air, the crystal data for complex **3** were collected on a crystal sealed in a glass-capillary tube containing mother-liquor. For this complex, large conformational disorder owing to rotation along the C–CF$_3$ bond axis was observed. Some peaks, not too far from a special position and not related to any of the already positioned atoms, were observed in difference maps. The peaks were attributed to a chloroform molecule and refined assuming an almost rigid group with a site occupation factor of 0.25, as suggested by the elemental analysis. The large values of the final *R* factor can be in part ascribed to the poor resolution of the solvent molecule but does not affect seriously the positions of the other atoms.

Crystal data for 1

$C_{24}H_{21}CoF_{12}N_2O_7$, $M = 736.36$, trigonal, space group $P3_1$ (no. 144), $a = 11.295(3)$, $b = 11.294(2)$, $c = 20.570(6)$ Å, $U = 2271.8(10)$ Å^3, $T = 293$ K, $Z = 3$, $D_c = 1.615$ g cm^{-3}, μ(Mo-Kα) = 0.685 mm^{-1}, 3413 unique reflections of which 2616 assumed as observed with $I > 2\sigma(I)$. Refinement on 420 parameters gave $R1 = 0.0433$, $R = 0.0682$ with $S = 1.045$.

Crystal data for 2

$C_{24}H_{21}CoF_{12}N_2O_6$, $M = 720.36$, trigonal, space group $P3_2$ (no. 145), $a = 11.249(1)$, $b = 11.254(4)$, $c = 20.307(6)$ Å, $U = 2227.5(10)$ Å^3, $T = 293$ K, $Z = 3$, $D_c = 1.611$ g cm^{-3}, μ(Mo-Kα) = 0.694 mm^{-1}, 3711 unique reflections of which 3179 assumed as observed with $I > 2\sigma(I)$. Refinement on 411 parameters gave $R1 = 0.0515$, $R = 0.0675$ with $S = 1.108$.

Crystal data for 3

$C_{24}H_{21}F_{12}MnN_2O_6 \cdot 0.25CHCl_3$, $M = 716.36$, monoclinic, space group $C2/c$ (no. 15), $a = 27.342(4)$, $b = 13.973(4)$, $c = 22.922(3)$ Å, $\beta = 125.79(1)°$, $U = 2227.5(10)$ Å^3, $T = 293$ K, $Z = 8$, $D_c = 1.395$ g cm^{-3}, μ(Mo-Kα) = 0.526 mm^{-1}, 4896 unique reflections of which 2230 assumed as observed with $I > 2\sigma(I)$. Refinement on 397 parameters and 3 restraints gave $R1 = 0.107$ with $S = 1.045$.

CCDC reference number 186/2107.

See http://www.rsc.org/suppdata/dt/b0/b004244g/ for crystallographic files in .cif format.

Acknowledgements

Financial support of the EU network 3MD (ERB 4061 PL 97-0197) is gratefully acknowledged.

References

1 R. D. Willett, R. M. Gaura and C. P. Landee, in *Extended Linear Chain Compounds*, ed. J. S. Miller, Plenum Press, New York, 1983, vol. 3, p. 143.
2 W. E. Hatfield, W. E. Ester, W. E. Monsh, M. W. Pickeus, L. W. ter Haar and R. R. Weller, in *Extended Linear Chain Compounds*, ed. J. S. Miller, Plenum Press, New York, 1983, vol. 3, p. 42.
3 L. J. de Jongh and A. R. Miedema, *Adv. Phys.*, 1974, **1**, 23.
4 P. M. Richards, in *Local Properties at Phase Transitions*, eds. K. A. Müller and A. Rigamonti, Editrice Compositori, Bologna, 1976, p. 359.
5 A. Bencini and D. Gatteschi, *EPR of Exchanged Coupled Systems*, Springer Verlag, Berlin, 1990.
6 L. J. de Jongh, in *Magnetic Structural Correlations in Exchange Coupled Systems*, eds. R. D. Willett, D. Gatteschi and O. Kahn, NATO ASI Series 140, Riedel, Dordrecht, 1985, p. 1.
7 F. D. M. Haldane, *Phys. Rev. Lett.*, 1983, **50**, 1153.
8 H. Kobayashi, *Acta Crystallogr., Sect. B*, 1978, **34**, 2818.
9 S. Sachdev, *Science*, 2000, **288**, 475.
10 M. T. Hutchings, G. Shirane, R. J. Birgeneau and S. L. Holt, *Phys. Rev. B*, 1972, **5**, 1999.
11 A. Caneschi, D. Gatteschi, P. Rey and R. Sessoli, *Inorg. Chem.*, 1988, **27**, 1756.
12 A. Caneschi, D. Gatteschi, J. P. Renard, P. Rey and R. Sessoli, *Inorg. Chem.*, 1989, **28**, 3314.
13 A. Gleizes and M. Verdaguer, *J. Am. Chem. Soc.*, 1981, **103**, 7373.
14 A. Meyer, A. Gleizes, J. J. Girerd, M. Verdaguer and O. Kahn, *Inorg. Chem.*, 1982, **21**, 1729.

15 J. P. Renard, M. Verdaguer, L. P. Regnault, W. A. C. Erkelens, J. Rossat-Mignod, J. Ribas, W. G. Stirling and C. Vettier, *J. Appl. Phys.*, 1988, **63**, 3538.
16 A. Caneschi, D. Gatteschi, P. Rey and R. Sessoli, *Acc. Chem. Res.*, 1989, **22**, 392.
17 D. Gatteschi and P. Rey, in *Magnetic Properties of Organic Materials*, ed. P. Lahti, Marcel Dekker, New York, 1999, p. 601.
18 A. Caneschi, D. Gatteschi, M. C. Melandri, P. Rey and R. Sessoli, *Inorg. Chem.*, 1990, **29**, 4228.
19 A. Caneschi, D. Gatteschi, J. Laugier, P. Rey, R. Sessoli and C. Zanchini, *J. Am. Chem. Soc.*, 1988, **110**, 2795.
20 C. I. Cabello, A. Caneschi, R. L. Carlin, D. Gatteschi, P. Rey and R. Sessoli, *Inorg. Chem.*, 1990, **29**, 2582.
21 A. Caneschi, F. Ferraro, D. Gatteschi, P. Rey and R. Sessoli, *Inorg. Chem.*, 1991, **30**, 3162.
22 A. Caneschi, F. Ferraro, D. Gatteschi, P. Rey and R. Sessoli, *Inorg. Chem.*, 1990, **29**, 4217.
23 D. Luneau, G. Risoan, P. Rey, A. Grand, A. Caneschi and D. Gatteschi, *Inorg. Chem.*, 1993, **32**, 5616.
24 F. L. de Panthou, D. Luneau, R. Musin, L. Öhrström, A. Grand, P. Turek and P. Rey, *Inorg. Chem.*, 1996, **35**, 3484.
25 A. Caneschi, D. Gatteschi and P. Rey, *Prog. Inorg. Chem.*, 1991, **39**, 331.
26 A. Caneschi, D. Gatteschi, P. Rey and R. Sessoli, *Inorg. Chem.*, 1991, **30**, 3936.
27 A. Caneschi, D. Gatteschi, J. Laugier and P. Rey, *J. Am. Chem. Soc.*, 1987, **109**, 2191.
28 A. Caneschi, D. Gatteschi, J. Laugier, R. Sessoli, P. Rey and C. I. Cabello, *J. Mater. Chem.*, 1992, **2**, 1283.
29 D. Gatteschi, J. Laugier, P. Rey and C. Zanchini, *Inorg. Chem.*, 1987, **26**, 938.
30 Z.-H. Jiang, Q. Yi, D.-Z. Liao, Z. W. Huan, S. P. Yan, G.-L. Wang, X.-K. Yao and R.-J. Wang, *Transition Met. Chem.*, 1995, **20**, 136.
31 A. Caneschi, D. Gatteschi, J. Laugier, L. Pardi and C. Zanchini, *Inorg. Chem.*, 1988, **27**, 2027.
32 A. Caneschi, D. Gatteschi, J. P. Renard, P. Rey and R. Sessoli, *Inorg. Chem.*, 1989, **28**, 1976.
33 K. Fegy, D. Luneau, T. Ohm, C. Paulsen and P. Rey, *Angew. Chem., Int. Ed.*,1998, **37**, 1270.
34 A. Caneschi, D. Gatteschi and A. le Lirzin, *J. Mater. Chem.*, 1994, **4**, 319.
35 J. Seiden, *J. Phys. Lett.* (*Paris*), 1983, **44**, L947.
36 A. Altomare, M. C. Murla, M. Camalli, G. Cascarano, C. Giacovazzo, A. Guagliardi, G. Polidori, R. Spagna and D. Viterbo, *J. Appl. Chem.*, 1989, **22**, 389.
37 G. M. Sheldrick, SHELXL-93, Program for Crystal Structure Refinement, University of Göttingen, Göttingen, 1993.